Energy Storage and Fluctuations in a Central-Spin Quantum Battery with Nearest-Neighbour Interactions

O.C. Kokkedee[1]

Applied Physics and Applied Mathematics, Delft University of Technology
Lorentzweg 1, 2628 CD Delft

Thesis Committee:

Dr. M. Blaauboer,	Supervisor
Dr. J.L.A. Dubbeldam,	Supervisor
Prof. Dr. Y.M. Blanter,	
Dr. J. Thies,	

March 12, 2024

TU Delft

Abstract

In this thesis the stored energy and its fluctuations of a central spin battery with nearest-neighbour interactions between the battery spins are investigated. Using analytical expressions, it is shown that for 2 battery spins and equal strength in the flip-flop interaction g and nearest-neighbour interaction J, the fluctuations are minimal whenever the battery is maximally charged when taking at least four charge spins. Similarly, whenever the formed envelopes of the energy have a zero, the fluctuations have a global maximum. In the same limit, it could also be seen that an increase of the charge spins N_c and spin-ups m, resulted in a higher global maximum of the stored energy. Furthermore for 2 battery spins, taking the limit $J \gg g$ results in a situation where the battery cannot be charged at all, whereas taking the limit $g \gg J$ results in a central spin battery where no nearest-neighbour interactions are present; its stored energy as a function of time is a single cosine function, that is always able to reach its theoretical maximum.
Similar results were found for systems with more than 2 battery spins. Increasing J with constant g resulted in a decrease of the global maximum of the energy, dropping from its theoretical maximum to its minimum. Opposite behaviour could be seen when increasing g with constant J. Whenever the global maximum of the energy crossed the line $E = 0$, the fluctuations at the same moment in time formed a peak.

Contents

Chapter 1

Introduction

It is only around a century ago when people found out that the classical laws we humans experience in our daily lives do not apply at the level of subatomic particles. Great physicists, such as Werner Heisenberg and Albert Einstein, laid the foundation of quantum theory, such as the unexpected behaviour of the electron: from uncertainty in position and velocity, to both particle and wave-like behaviour. With the basis of quantum theory, a whole new branch of physics was yet to be discovered.
Many phenomena within quantum theory were compared with its classical counterparts. An important example was the quest to find similar applications of thermodynamics in the quantum world. Classical thermodynamics was found to be useful for already a long time due to its description of systems with an extremely large amount of particles in only a small number of macroscopic quantities. The question arose how the simplification of systems containing those amounts of particles could be translated to the quantum world. In the classical and quantum world, average values are used to describe systems. However, when decreasing the size of a classical system, thermal fluctuations in these quantities are noticeable. These are present in the quantum regime as well, but in this case these fluctuations mainly have a quantum origin [9]. Possible applications of quantum thermodynamics that are studied theoretically are e.g. quantum thermal machines, quantum refrigerators and quantum batteries. They all have a similar purpose as their classical counterpart, but their mechanism is based on quantum phenomena [9].
A quantum battery is a quantum system in which energy can be stored, which can be extracted in the form of work. They are of high interest due to their possible high performance compared to their classical counterparts, i.e. faster charging time and potential loss-free storage [6]. In this thesis, a so-called central-spin quantum battery is considered. This is a quantum battery based on the central spin model [1], a theoretical model that can be calculated exactly and can be realised by e.g. quantum dots [10, 11].
A central-spin battery consists of a battery part, containing N_b central-spins, and a charge part, with N_c bath-spins. Central spins, from now denoted as battery spins, serve as the battery's core components, responsible for storing and transferring energy within the system. On the other hand, bath spins, designated as charge-spins, act as the energy source, interacting with the battery spins through the flip-flop interaction. This interaction results in the interchange of the quantum state of the two interacting spins. Both battery- and charge-spins are spin-1/2 particles. If the battery-spins are prepared such that all of them are spin-down, and charge-spins are prepared such that a number of them are spin-up, then the charge-spins are able to elevate the battery-spins to an

excited state. In this way, the charger spins 'charge' the battery spins, as the increase of energy within the battery part of the system can be used later in the form of extracted work.
In the model described in this report, also nearest-neighbour interactions between the battery spins are present. It is a type of coupling that only occurs between two nearest-neighbour battery spins. This distinction separates the flip-flop interaction from the nearest-neighbor interaction, as the former operates between any battery and charge spin. Research on the influence of the nearest-neighbour interactions includes the impact on the stable energy [4] and the charging process [12] of a quantum battery. The following figure contains a model of a central spin quantum battery, with indications in what direction the different interactions act. See the caption for more information.

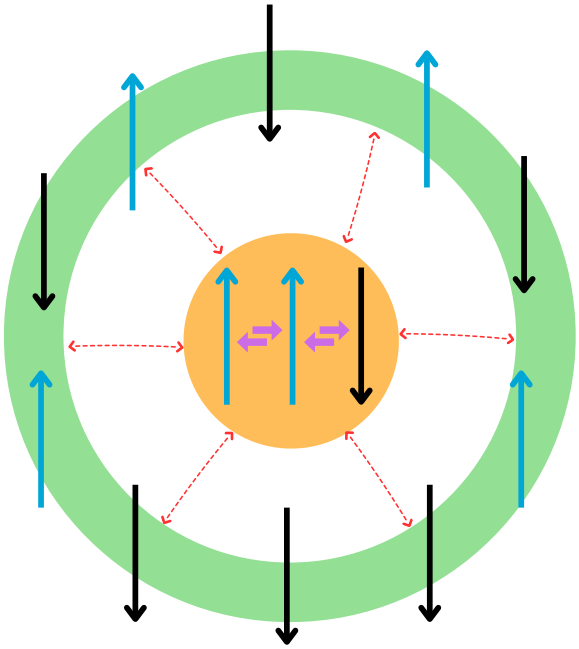

Figure 1.1: This figure illustrates the mechanics of a central spin quantum battery. It contains a battery part (orange circle) and charge part (green ring). Spin-up states are represented by a blue arrow and spin-down states by a black arrow. The battery spins interact with the charge spin by means of the flip-flop interaction (red arrows). This takes place between any pair of battery and charge spin. The battery spins interact with each other as well by means of the nearest-neighbour interaction (purple arrows). This only takes place between two consecutive spins.

In quantum mechanics, while certainty is attainable under specific conditions, Heisenberg's uncertainty principle emphasizes the general uncertainty in quantum phenomena. As the stored energy within the battery is established by means of quantum phenomena, it has an uncertainty as well and thus there exist fluctuations in the stored energy. These are undesired as they would reduce the performance of quantum batteries, i.e. incomplete charging and reduction of the charging power [3].

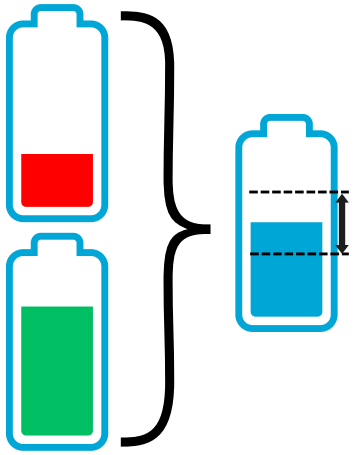

Figure 1.2: A quantum battery can be in a superposition of different states (left two batteries). This results in fluctuations of the energy, which is illustrated on the right.

It is the goal of this project to investigate the stored energy E and its fluctuations Σ^2 of a central-spin battery, which battery spins experience nearest-neighbour interactions. Both quantities can be computed using well known tools in quantum theory, such as the Hamiltonian and the density matrix. However, all concepts will be explained and the calculations are done step-by-step. For this, the report is structured as follows: chapter 2 contains the theoretical framework necessary for the calculations of the stored energy and its fluctuations. This chapter starts with section 2.1, which describes important concepts and properties of spin-1/2 systems, such as the spin operators and its eigenstates. This will be done for both individual spin-1/2 particles and multiple particle systems. Section 2.2 introduces the Hamiltonian and (reduced) density matrix, and shows how these can be used to compute E and Σ^2. The final section 2.3 of chapter 2 the Hamiltonian of a central-spin quantum battery is given and the method of finding the reduced density matrix of a quantum system using the given Hamiltonian is shown. The results in chapter 3 consists of two parts. The first, section 3.1, shows analytical calculations for a CSQB with 2 battery spins. This is the only case for which solutions could be calculated in an exact fashion. To extend these results to a larger system with more than 2 battery spins, numerical calculations were used of which the results are given in section 3.2.

Chapter 2

Theoretical Framework

2.1 Spin-1/2 Systems

As the quantum battery described in this thesis is a central-spin battery, it is important to introduce spin-$\frac{1}{2}$ systems. An introduction will be given on spin, the associated Pauli matrices and their corresponding eigenvectors and eigenvalues. Initially, only single spin-$\frac{1}{2}$ particles are considered, after which the discussed concepts will be extended to multiple particle systems.
It is important to note that in this report $\hbar = 1$. So for the calculations, natural units have been used.

2.1.1 Spin-1/2 Particles and Their States

Spin-$\frac{1}{2}$ systems consists of spin-$\frac{1}{2}$ particles. These particles have spin number $s = \frac{1}{2}$ with an associated quantum spin number m_s. For m_s we have $m_s \in \{\frac{1}{2}, -\frac{1}{2}\}$, where the values correspond with a different orientation of the spin. $\frac{1}{2}$ corresponds with spin-up and $-\frac{1}{2}$ with spin-down. In nature, the class of particles that have spin-$\frac{1}{2}$ are called fermions.
There are different notations to write the eigenstates of systems. It is possible to do this using vectors or bra-ket notation. I.e. we can denote spin-up and spin-down states respectively as

$$|\uparrow\rangle = \begin{pmatrix} 1 \\ 0 \end{pmatrix} \quad \text{and} \quad |\downarrow\rangle = \begin{pmatrix} 0 \\ 1 \end{pmatrix}. \tag{2.1}$$

Important matrices associated with spin-$\frac{1}{2}$ particles are the famous Pauli matrices. They are given by

$$\sigma^x \equiv \begin{pmatrix} 0 & 1 \\ 1 & 0 \end{pmatrix}, \quad \sigma^y \equiv \begin{pmatrix} 0 & -i \\ i & 0 \end{pmatrix}, \quad \sigma^z \equiv \begin{pmatrix} 1 & 0 \\ 0 & -1 \end{pmatrix}. \tag{2.2}$$

Using the Pauli matrices, one can get the spin operators using the expression

$$s^\alpha \equiv \frac{\hbar}{2}\sigma^\alpha = \frac{1}{2}\sigma^\alpha, \qquad \alpha \in \{x, y, z\} \tag{2.3}$$

Spin operators important for this thesis are the ladder operators, given by $s^\pm = s^x \pm i s^y$. As the spin up and down states are defined in the z-direction, it follows that the s^z operator gives the energy value of the given state: $s^z |\uparrow\rangle = \frac{1}{2}|\uparrow\rangle$ and $s^z |\downarrow\rangle = -\frac{1}{2}|\downarrow\rangle$,

which means $\pm\frac{1}{2}$ are the eigenvalues of the eigenstates $|\uparrow\rangle$ and $|\downarrow\rangle$.
The σ^+ operator increases the quantum spin number of a state by 1, while the s^- operator decreases the quantum number by the same amount. It also gives the energy level splitting between both states: $s^+ |\downarrow\rangle = |\uparrow\rangle$ and $s^- |\uparrow\rangle = |\downarrow\rangle$. Note, however, that s^+ returns zero if it operates on spin-up state, as the state can not be any higher. Idem for s^- but for the lowest possible state.

2.1.2 Tensor Product

An important mathematical operation for the construction of bases with multiple particles is the tensor product. It is used to construct the Hilbert space of composite quantum systems. When applying the operation on a $m \times n$ matrix $\boldsymbol{A}$ and $p \times q$ matrix $\boldsymbol{B}$, a $mp \times nq$ matrix is formed given by:

$$\boldsymbol{A} \otimes \boldsymbol{B} = \begin{bmatrix} a_{11}\boldsymbol{B} & \cdots & a_{1n}\boldsymbol{B} \\ \vdots & \ddots & \vdots \\ a_{m1}\boldsymbol{B} & \cdots & a_{mn}\boldsymbol{B} \end{bmatrix}. \tag{2.4}$$

When applying it on a n-dimensional vector $\boldsymbol{v}$ and m-dimensional vector w, we get the following product mn-dimensional vector:

$$\boldsymbol{v} \otimes \boldsymbol{w} = \begin{bmatrix} v_1\boldsymbol{w} \\ v_2\boldsymbol{w} \\ \vdots \\ v_n\boldsymbol{w} \end{bmatrix} \tag{2.5}$$

When the tensor-product is applied on two quantum systems, it is applied on the bases of these systems, and thus its eigenstates. To demonstrate this, suppose we have two Hilbert subspaces $\mathcal{A}$ and $\mathcal{B}$. The two spaces combined using the tensor product produces another Hilbert subspace $\mathcal{A} \otimes \mathcal{B}$. Its states are given by

$$|\alpha\rangle \otimes |\beta\rangle = |\alpha\rangle\,|\beta\rangle\,, \qquad |\alpha\rangle \in \mathcal{A},\ |\beta\rangle \in \mathcal{B}.$$

The tensor product will be used to construct the basis used for this research.

2.1.3 Multiple Particle Systems

When considering systems with multiple particles, there are various options for selecting bases for the eigenstates. One common choice is the standard basis, which serves as a foundation for constructing other bases. For instance, in a quantum system containing a single spin-$\frac{1}{2}$ particle, the standard basis is $\{(1\ 0)^T, (0\ 1)^T\}$. However, for this thesis, an alternative basis has been used, namely a reduced one (this will be explained further shortly). The motivation behind this decision lies in the impracticality of the standard basis due to its exponential growth in size. In a system composed of N spin-$\frac{1}{2}$ particles, the standard basis expands to a size of 2^N, making calculations inconvenient for larger systems. Therefore, picking a different basis is desired, as it may simplify calculations for other quantities essential to this thesis.
To keep the amount of calculations tractable, we can consider a subspace that contains

all states that are symmetric under the exchange of particles, the so-called Dicke-states. Consider N particles of which m have spin-up. The Dicke state describing this system is given by

$$|m\rangle \equiv \frac{1}{\sqrt{\binom{N}{m}}} \sum_k P_k(|\uparrow_1, \cdots, \uparrow_m, \downarrow_{m+1}, \cdots, \downarrow_N\rangle), \tag{2.6}$$

where $\binom{N}{m} = N!/[m!(N-m)!]$ and P_k is the notation for all distinct permutations of the given state. A basis used for a system containing N particles, spanned by Dicke states only increases with size $N+1$. This is much smaller compared to the standard basis. It is also to be expected, as the standard basis contains each individual permutation when distributing m spin-ups over N spins. When describing all of these permutation as a single state, a Dicke state, the size of the basis is reduced dramatically.
As the central spin battery contains multiple battery and charge spins, we must define the spin-operators for multiple particle systems. For N particles, the spin-operators are defined as

$$S^\alpha = \sum_{j=1}^{N} s_j^\alpha \qquad \alpha \in \{x, y, z\}, \tag{2.7}$$

where s_j^α is the spin operator of type α acting on particle j.
Suppose there are N spin-1/2 particles present, of which m have spin up. In that case, the spin number is given by $s = N/2$ and the quantum spin number is given by $m_s = m/2 - (m-N)/2 = m - N/2$. In that case the necessary spin operators for this these are given by:

$$\begin{aligned}
S^z |m\rangle_N &= (m - \frac{N}{2}) |m\rangle_N , \\
S^+ |m\rangle_N &= \sqrt{\frac{N}{2}\left(\frac{N}{2}+1\right) - \left(m - \frac{N}{2}\right)\left(m - \frac{N}{2}+1\right)} |m+1\rangle_N , \\
S^- |m\rangle_N &= \sqrt{\frac{N}{2}\left(\frac{N}{2}+1\right) - \left(m - \frac{N}{2}\right)\left(m - \frac{N}{2}-1\right)} |m-1\rangle_N ,
\end{aligned} \tag{2.8}$$

with $|m+a\rangle$, $a \in \{1, 0, -1\}$ being Dicke states [5, p. 166-168].

2.2 Energy and Fluctuations of a Quantum System

In order to calculate the energy stored in a quantum system, and to find the fluctuations of the energy, there are some concepts that need to be discussed first. These concepts are the Hamiltonian of a quantum system, the reduced density matrix and how it can be found using the state of a quantum system. Eventually the formulas which compute the energy and fluctuations of a quantum system are given.

2.2.1 Density Matrix and Reduced Density Matrix

The density matrix is a convenient way of describing a mixed state of a quantum system. E.g. for a quantum battery with both battery and charge cells that interact with one another, it is impossible to describe the system by using only a single ket vector. In order

to still describe the system in a practical way, the density matrix comes in useful. It is also required to calculate the stored energy and its fluctuations.
The density matrix ρ is defined by

$$\rho = \sum_{i}^{N} p_i \left|\psi_i\right\rangle \left\langle\psi_i\right|, \tag{2.9}$$

where p_i is the probability that the system is in state $|\psi_i\rangle$.
Using the density matrix, one is able to easily calculate the expected value of an observable A within a system by the following formula

$$\langle A\rangle = \sum_{i}^{N} p_i \left\langle\psi_i\right| A \left|\psi_i\right\rangle = \mathrm{Tr}(\rho A), \tag{2.10}$$

with the trace of a $N \times N$ matrix A is given by

$$\mathrm{Tr}(A) \equiv \sum_{i=1}^{N} A_{ii}. \tag{2.11}$$

Furthermore, suppose a quantum system is composed of two systems A and B. Let ρ be the density matrix of the entire system. Then we can find the density matrix of only system A, called the reduced density matrix, by using the partial trace:

$$\rho_A = \mathrm{Tr}_B(\rho). \tag{2.12}$$

With the partial trace, one can filter out one subsystem to be left with the (reduced) density matrix of the other subsystem. This operation can be used when a system contains multiple subsystems as well. By tracing over the subsystems that are not of interest, one is left with the reduced density matrix of the desired subsystems [7].

2.2.2 Hamiltonian, Energy and Fluctuations

The Hamiltonian is a mathematical operator that is a key concept for quantum mechanics. It describes the energy of a quantum system, but also how a state of a system changes over time according to Schrödinger's equation:

$$i\hbar\frac{\partial}{\partial t}\left|\psi\right\rangle = H\left|\psi\right\rangle. \tag{2.13}$$

As mentioned in the previous section, the density matrix can be used to compute the expected value of an observable. As the Hamiltonian corresponds with the energy of a system, it may be clear that the stored energy of a quantum system E can be found by

$$E = \mathrm{Tr}(\rho H). \qquad [8] \tag{2.14}$$

The fluctuations Σ^2 of the stored energy can be computed as follows:

$$\Sigma^2 = \mathrm{Tr}(\rho H^2) - (\mathrm{Tr}(\rho H))^2. \qquad [3] \tag{2.15}$$

2.3 Central Spin Quantum Battery

In this section, the mathematical foundation of the central spin battery will be laid. First the Hamiltonian for this system will be given, after which it is shown how one can find the reduced density matrix, the stored energy and its fluctuation using this Hamiltonian.

The total Hamiltonian H of a quantum battery consists of four sub-Hamiltonians. One that describes the nearest-neighbour interaction within battery part, one that describes the energy splitting of the battery part, one that describes the charge part and one that describes the interaction between the two systems. Suppose one has N_b battery spins, N_c charge spins and m total spins-up. Assume that $N_c \geq m \geq N_b$. Then the Hamiltonian is given by:

$$\begin{aligned} H &= H_b^0 + H_b' + H_c + H_{b-c} \\ H_b^0 &= \frac{\omega_b}{2} S_b^z \\ H_b' &= J \sum_{i=1}^{N_b-1} \left(s_i^+ s_{i+1}^- + s_i^- s_{i+1}^+ \right) \\ H_c &= \frac{\omega_c}{2} S_c^z \\ H_{b-c} &= g \left(S_b^+ S_c^- + S_b^- S_c^+ \right) \end{aligned} \tag{2.16}$$

where $\omega_{b,c}/2$ is the energy splitting of the battery and charge spins, J is the strength of the nearest-neighbor interaction between the battery spins, g is the strength of the flip-flop interaction between the battery and charge spins, and the $S_{b,c}^\alpha$ and s_b^α are the spin operators as given in Eq. (2.3) and (2.8).
The quantum battery is prepared such that at $t = 0$ the battery part is in its ground state. This means that all battery cells are spin-down: $|0\rangle_b = |\downarrow_1, \downarrow_2, \cdots, \downarrow_{N_b}\rangle$. The charger is prepared with all m spin-ups and, if applicable, the rest of the cells spin-down. The corresponding state is $|m\rangle_c$, which is defined as in 2.6. This gives the initial state $|0\rangle_b \otimes |m\rangle_c = |0\rangle_b |m\rangle_c$. Assume that at all times, the total number of spin-ups of the whole system remains equal to m. From this it follows that, supposing the battery contains $j < m$ spins-up, the charger must contain $m - j$ spins-up resulting in the state $|j\rangle_b |m-j\rangle_c$. Going over all the possible combinations gives the basis

$$\mathcal{H}_m = \{|0\rangle_b |m\rangle_c, |1\rangle_b |m-1\rangle_c, \cdots, |N_b\rangle_b |m-N_b\rangle_c\}. \tag{2.17}$$

We can write the Hamiltonian in matrix form, which is more convenient than the form in Eq. (2.16). We find for the Hamiltonian:

$$H = \begin{pmatrix} b_0 & u_1 & & & & \\ u_1 & b_1 + n_1 J & u_2 & & & \\ & \ddots & \ddots & & \ddots & \\ & & u_{N_b-1} & b_{N_b-1} + n_{N_b-1} J & u_{N_b} & \\ & & & u_{N_b} & b_{N_b} & \end{pmatrix} \tag{2.18}$$

where n_j is the total number of contributions J by the Dicke state $|j\rangle_b$ and u_j and b_j are given by

$$\begin{aligned} u_j &= \langle m-j|_c\langle j|_b \left(H_{b-c}\right)|j-1\rangle_b|m-j+1\rangle_c = \langle m-j+1|_c\langle j-1|_b \left(H_{b-c}\right)|j\rangle_b|m-j\rangle_c \\ &= g\sqrt{j(N_b-j+1)(N_c-m+j)(m-j+1)}, \\ b_j &= \langle m-j|_c\langle j|_b \left(H_b^0+H_c\right)|j\rangle_b|m-j\rangle_c = \frac{\omega_b}{2}(j-\frac{N_b}{2})+\frac{\omega_c}{2}(m-j-\frac{N_c}{2}). \end{aligned} \tag{2.19}$$

The coefficients u_i and b_i are found using the spin operators stated in Eq. (2.8) and performing the bra-ket calculations shown in Eq. (2.19). The Hamiltonian and its coefficients are similar to the one given by Liu et al. [8], except it now contains nearest-neighbour interaction terms.

As mentioned, n_j is the total number of contributions J by the Dicke state $|j\rangle_b$. It is the number of reversals in a given quantum state, taking into account all the possible combinations for the given state and is a result of the summation in H_b' in Eq. (2.16) and the summation over all possible combinations, given in the Dicke state Eq. (2.6). In this case, by "reversal," we mean when two nearest-neighbour battery spins are opposite oriented, so when we have $[\uparrow\downarrow]$ or $[\downarrow\uparrow]$, where the two arrows are nearest-neighbour spins. n_j can be found as follows: take for example the Dicke state $|2\rangle_b$ with $N=4$. The $\binom{4}{2}=6$ possible combinations of this state are

1. $[\uparrow\uparrow\downarrow\downarrow] \quad \rightarrow \quad n_{\text{rev}}=1$
2. $[\uparrow\downarrow\uparrow\downarrow] \quad \rightarrow \quad n_{\text{rev}}=3$
3. $[\uparrow\downarrow\downarrow\uparrow] \quad \rightarrow \quad n_{\text{rev}}=2$
4. $[\downarrow\uparrow\uparrow\downarrow] \quad \rightarrow \quad n_{\text{rev}}=2$
5. $[\downarrow\uparrow\downarrow\uparrow] \quad \rightarrow \quad n_{\text{rev}}=3$
6. $[\downarrow\downarrow\uparrow\uparrow] \quad \rightarrow \quad n_{\text{rev}}=1$

where the total number of reversals n_{rev} of each state is given next to the respective state. In this case, the number of contributions is $n_2=\sum_i n_{\text{rev},i}=12$. If N is small, the number of contributions can still be calculated by hand. For larger N, however, the number of combinations and thus values of n_j become quite large, so it can be only computed using a computer program.

Now that we have found a matrix description of H, we can diagonalize it to obtain the form $H=UDU^\dagger$, where U is an unitary matrix and D a diagonal matrix. The wave function of the entire system can be found by writing $\boldsymbol{\psi}(t)=Ue^{-iDt}U^\dagger(1\ 0\ \ldots\ 0)^T$. Since we are only interested in the stored energy and fluctuations in the battery spins, we need the reduced density matrix of the battery part of the system. We can find this using the wave function and the following expression:

$$\begin{aligned} \rho_b(t) &= \text{Tr}_c(|\boldsymbol{\psi}(t)\rangle\langle\boldsymbol{\psi}(t)|) \\ &= |\psi_1(t)|^2|0\rangle\langle 0| + \cdots + |\psi_{N_b+1}(t)|^2|N_b\rangle\langle N_b|. \end{aligned} \tag{2.20}$$

From the definition one can see that the reduced density matrix is a diagonal matrix. It has the characteristic that each element shows the occupation of its corresponding

state: ρ_{11} is the probability of finding the system in the first state, or the state where all battery spins are spin-down. ρ_{22} has a similar definition, except it is for the state where one battery spin has spin-up. This continues for the diagonal elements of the matrix until $\rho_{N_bN_b}$, which is the probability of having all battery spins spin-up.
Finally, the stored energy and the fluctuations in the battery part of the system can be found by the following expressions [8, 3]:

$$\begin{aligned} E_b(t) &= \mathrm{Tr}(H_b^0 \rho_b(t)), \\ \Sigma_b^2(t) &= \mathrm{Tr}((H_b^0)^2 \rho_b(t)) - (\mathrm{Tr}(H_b^0 \rho_b(t))^2, \end{aligned} \tag{2.21}$$

with H_b^0 being defined in matrix form as: $H_b^0 = \mathrm{Diag}\left(b'_0\ b'_1\ \dots\ b'_{N_b}\right)$, with $b'_j = \frac{\omega_b}{2}(j - N_b/2)$. Note that of the entire Hamiltonian H (2.16) only H_b^0 is in Eq. (2.21). This is because only the energy that is stored in the battery spins when they are in their excited states can be extracted in the form of work. Hence all other terms in H are neglected as they do not contribute any energy that can be counted as stored energy.

Chapter 3

Results

The results are split into two parts. The first part is the case $N_b = 2$. This is the only case of N_b where H can be diagonalized analytically, and thus where $\rho_b(t)$, $E_b(t)$ and $\Sigma_b^2(t)$ can be computed in an exact fashion. For $N_b > 2$, a python program is used to do similar analysis as done for $N_b = 2$.
To check whether the battery spins are all able to be spin-up at the same time when considering specific values for the parameters given in Eq. (2.18), we can calculate the theoretical maximal energy of a system. From the definition of the reduced density matrix, all battery spins are spin-up when $\rho_{N_bN_b}(t) = 1$. Call the reduced density matrix for this condition $\rho_b^{\max}$, which is given by

$$\rho_{ij}^{\max} = \begin{cases} 1 & \text{for} \quad i = j = N_b \\ 0 & \text{else} \end{cases} \tag{3.1}$$

In this manner we can calculate the maximum of the energy within the battery for general N_b. We have

$$E_b^{\max} = \mathrm{Tr}(\rho_b^{\max} H_b^0) = \frac{\omega_b N_b}{4}. \tag{3.2}$$

This means that the maximum of the stored energy is linear with the size of the battery part of the system. Furthermore, if $\rho_b(t) = \rho_b^{\max}$, then the fluctuations are equal to zero, because under these conditions we have

$$\mathrm{Tr}(\rho_b^{\max} H_b^2) = (\mathrm{Tr}(\rho_b^{\max} H_b^0))^2$$

It is important to understand the meaning of the result found in equation (3.2). There are multiple ways to interpret it, of which one is that it is the largest eigenvalue of the battery part of the system (so the largest eigenvalue of H_b^0). Another way it can be interpreted is that it is the theoretical maximum value that $E_b(t)$ as given in Eq. (2.21) can reach. As will be seen momentarily, the energy as function of time is in general a trigonometric function that has values above and below zero. $E_b^{\max}$ is the maximum possible value above zero of the energy.
A similar analysis can be done for the minimum possible energy. This is when the system is in its ground state, or when all the battery spins are spin-down, and thus $\rho_{11}(t) = 1$. In that case, the minimum energy $E_b^{\min}$ is given by

$$E_b^{\min} = -\frac{\omega_b N_b}{4} = -E_b^{\max} \tag{3.3}$$

As with the maximum energy, the fluctuations are zero when the battery is in its ground state.
To check whether these values are correct, we can compute $E_b^{\max}$ and $E_b^{\min}$ for $N_b = 1$, and calculate its difference:

$$E_b^{\max} - E_b^{\min} = \frac{\omega_b}{2},$$

which is equal to the energy splitting given in H_b^0 in Eq. (2.16).

3.1 Case $N_b = 2$

In order to simplify the calculations, assume that $\omega_b = \omega_c \equiv \omega$. Then $b_1 = b_2 = b = \omega/2(m - 1 - N_c/2)$. H and H_b^0 are given by

$$H = \begin{pmatrix} b & u_1 & 0 \\ u_1 & b+2J & u_2 \\ 0 & u_2 & b \end{pmatrix}, \qquad H_b^0 = \frac{\omega}{2}\begin{pmatrix} -1 & 0 & 0 \\ 0 & 0 & 0 \\ 0 & 0 & 1 \end{pmatrix}. \tag{3.4}$$

Here u_1, u_2 and b are defined as in Eq. (2.19).
To calculate the reduced density matrix $\rho_b(t)$, we use the method described in the previous section. We start of by diagonalizing H such that $H = UDU^\dagger$.
We find $D = \mathrm{Diag}(\lambda_1\ \lambda_2\ \lambda_3)$, where

$$\begin{aligned} \lambda_1 &= b, \\ \lambda_2 &= b + J - \sqrt{J^2 + u_1^2 + u_2^2}, \\ \lambda_3 &= b + J + \sqrt{J^2 + u_1^2 + u_2^2}. \end{aligned} \tag{3.5}$$

Write $A \equiv J^2 + u_1^2 + u_2^2$. We find for U:

$$U = \frac{1}{\sqrt{2\sqrt{A}\,(A - J^2)}} \begin{bmatrix} \sqrt{2\sqrt{A}}u_2 & u_1\sqrt{\sqrt{A}+J} & u_1\sqrt{\sqrt{A}-J} \\ 0 & \left(J-\sqrt{A}\right)\sqrt{\sqrt{A}+J} & \left(J+\sqrt{A}\right)\sqrt{\sqrt{A}-J} \\ -\sqrt{2\sqrt{A}}u_1 & u_2\sqrt{\sqrt{A}+J} & u_2\sqrt{\sqrt{A}-J} \end{bmatrix} \tag{3.6}$$

The eigenvectors of H are normalized in such a way that all the vectors share a common factor of $1/\sqrt{2\sqrt{A}(A - J^2)}$.
For the wavefunction of the entire system $\boldsymbol{\psi}(t)$, we find:

$$\boldsymbol{\psi}(t) = \frac{1}{2\sqrt{A}\,(A - J^2)} \begin{bmatrix} 2\sqrt{A}u_2^2 e^{-i\lambda_1 t} + u_1^2\left[\left(\sqrt{A}+J\right)e^{-i\lambda_2 t} + \left(\sqrt{A}-J\right)e^{-i\lambda_3 t}\right] \\ \left(A - J^2\right)u_1\left(e^{-i\lambda_3 t} - e^{-i\lambda_2 t}\right) \\ u_1u_2\left[-2\sqrt{A}e^{-i\lambda_1 t} + \left(\sqrt{A}+J\right)e^{-i\lambda_2 t} + \left(\sqrt{A}-J\right)e^{-i\lambda_3 t}\right] \end{bmatrix} \tag{3.7}$$

Using the expression given in Eq. (2.20), we find for ρ_b:

$$\rho_b(t) = \rho_{11}(t)|0\rangle\langle 0| + \rho_{22}(t)|1\rangle\langle 1| + \rho_{33}(t)|2\rangle\langle 2| \tag{3.8}$$

where

$$\begin{aligned}
\rho_{11}(t) &= \frac{1}{A\left(A-J^2\right)^2}\left\{Au_2^4 + u_1^4\left[J^2 + \left(A-J^2\right)\cos^2(\sqrt{A}t)\right]\right. \\
&\quad \left. + \sqrt{A}u_1^2u_2^2\left[\left(\sqrt{A}+J\right)\cos\left(\left(\sqrt{A}-J\right)t\right) + \left(\sqrt{A}-J\right)\cos\left(\left(\sqrt{A}+J\right)t\right)\right]\right\} \\
\rho_{22}(t) &= \frac{u_1^2}{A}\left(1-\cos^2\left(\sqrt{A}t\right)\right) \\
\rho_{33}(t) &= \frac{u_1^2u_2^2}{A\left(A-J^2\right)^2}\left\{A + J^2 - \sqrt{A}\left[\left(\sqrt{A}+J\right)\cos\left(\left(\sqrt{A}-J\right)t\right) + \left(\sqrt{A}-J\right)\cos\left((\sqrt{A}+J)t\right)\right]\right. \\
&\quad \left. + \left(A-J^2\right)\cos^2\left(\sqrt{A}t\right)\right\}.
\end{aligned} \tag{3.9}$$

$\rho_{11}(t)$ is the probability of finding the battery in the ground state (both battery spins are spin-down) at time t, $\rho_{22}(t)$ is the probability of finding the battery such that one battery spin is spin-up and the other is spin-down at time t and $\rho_{33}(t)$ is the probability that both battery spins are spin-up.
When substituting $J = 0$ in Eq. (3.9), the same result is obtained as found by Liu et al. [8]. Furthermore, $\sum_{i=1}^{3}\rho_{ii}(t) = 1$ for all t, $\rho_{11}(0) = 1$ and $\rho_{22}(0) = \rho_{33}(0) = 0$.
Using these coefficients we can calculate the stored energy and its fluctuations with

$$\begin{aligned}
E_b(t) &= \frac{\omega}{2}(\rho_{33}(t) - \rho_{11}(t)) \\
\Sigma^2(t) &= \frac{\omega^2}{4}(\rho_{11}(t)(1-\rho_{11}(t)) + \rho_{33}(t)(1-\rho_{33}(t))) + \omega\rho_{33}(t)\rho_{11}(t)
\end{aligned} \tag{3.10}$$

Unfortunately, the expressions for $\rho_b(t)$ are quite long with inconvenient terms for general J, g, N_c and m. The expressions only get worse once we fill them in Eq. (3.10). However, the formulas for these last two quantities reduce to simpler expressions if we let $u_1 = u_2 \equiv u$. This is the case for $N_c = 2(m-1)$, where we can choose any $m \geq 2$. In that case, the fluctuations and energy expressions reduce to

$$\begin{aligned}
E_b(t) &= -\frac{\omega}{4\sqrt{A}}\left[\left(\sqrt{A}+J\right)\cos\left(\left(\sqrt{A}-J\right)t\right) + \left(\sqrt{A}-J\right)\cos\left(\left(\sqrt{A}+J\right)t\right)\right] \\
\Sigma_b^2(t) &= \frac{\omega^2}{4A}\left(u^2 + J^2 + u^2\cos^2\left(\sqrt{A}t\right)\right) - E_b(t)^2 \\
&= \frac{\omega^2}{32A}\left(4A - 2\left(A-J^2\right)\cos(2Jt) - \left(\sqrt{A}+J\right)^2\cos\left(2\left(\sqrt{A}-J\right)t\right)\right. \\
&\qquad \left. - \left(\sqrt{A}+J\right)^2\cos\left(2\left(\sqrt{A}+J\right)t\right)\right)
\end{aligned} \tag{3.11}$$

$E_b(t)$ has extrema at $t = \frac{j\pi}{\sqrt{A}}$ and $t = \frac{\pi}{2J}(1+2j)$. Only the values $t = \frac{j\pi}{\sqrt{A}}$ are also extrema for the fluctuations. Unfortunately, these extrema are not consistent in terms of maxima and minima. The extrema alternate between maxima and minima for different values of j, but this also happens for the same values of j and different values of N_c and m.

3.1.1 Special Case $J = g \equiv h$

Using the constraint $N_c = 2(m-1)$ we can find even simpler expressions than given in Eq. (3.11), if we consider the case $J = g \equiv h$. When we substitute $N_c = 2(m-1)$ in

$u^2 = 2m(N_c - m + 1)h^2$, we get $u^2 = 2(m^2 - m)h^2$. We know furthermore, if $J = g = h$, that $A = (2M + 1)h^2$, where

$$M \equiv \frac{u^2}{g^2} = \frac{u^2}{h^2} = \left(\sqrt{2m(N_c - m + 1)}\right)^2. \tag{3.12}$$

Notice that $M = 2(m^2 - m)$. We obtain $2M + 1 = 4m^2 - 4m + 1$. Finally, using the transformation $m \to n + 1$, $n \in \mathbb{N}$, we get $2M + 1 = 4m^2 - 4m + 1 = 4n^2 + 4n + 1 = (2n + 1)^2 = k^2$, $k \in \mathbb{N}$. This means that A can be written as $A = k^2h^2$ for

$$\begin{cases} m = n + 1 \\ N_c = 2(m - 1) = 2n \qquad n \in \mathbb{N} \\ k = 2n + 1 \end{cases} \tag{3.13}$$

For the rest of this section, so for all results where $N_b = 2$, mostly n and k will be used to describe the size of the systems (N_c and m) and will be put on axes of figures. This has been done for several reasons. Of course, N_c and m have a clear physical interpretation, but when choosing one of those, one might forget that these both increase or decrease simultaneously. This is because for the rest of this section, we keep using the simplification $u_1 = u_2 = u$ which only suffices for the values given in Eq. (3.13). When taking n or k and increase it, it is clear that both m and N_c increase. Furthermore, k is found in many expressions to come, so it is more convenient to use it in context as well. However, whenever necessary, the value of N_c or m is given as well to include a physical interpretation to the results for those cases.
Now, when calculating the fluctuations in the energy, we find

$$\begin{cases} E_b(t) = -\frac{\omega}{4k}\left((k+1)\cos((k-1)ht) + (k-1)\cos((k+1)ht)\right) \\ \Sigma^2(t) = \frac{\omega^2}{32k^2}\left(4k^2 - 2(k^2-1)\cos(2ht) - (k+1)^2\cos(2h(k-1)t) - (k-1)^2\cos(2h(k+1)t)\right) \end{cases} \tag{3.14}$$

$\Sigma^2(t)$ and $E_b(t)$ have global maxima at

$$t^E_{j,k} = \frac{\pi}{h}\left(j \pm \frac{1}{k}\right) \quad \text{and} \quad t^\Sigma_{j,k} = \frac{\pi}{h}(j + \frac{1}{2}(1 \pm \frac{1}{k})), \quad \text{for} \quad j \in \mathbb{Z}. \tag{3.15}$$

The values of the global maxima of $E_b(t)$ and $\Sigma^2_b(t)$ will be given and discussed shortly. These values show that both functions are periodic, with period $\frac{\pi}{h}$. $\Sigma^2_b(t)$ has a phase-difference of $\pi/(2h)$ compared to $E(t)$. More importantly, one can see that the battery gets charged faster when the system is increased in size (when k is increased) or when the nearest-neighbour and flip-flop coupling is increased, so when h is increased. The period does not change when increasing k, but the respective maximum gets closer to the fixed point in the period. This will be made more clear momentarily.
Filling in the found values of t in their corresponding quantity gives

$$\begin{aligned} \Sigma^2(t^\Sigma_{0,k}) &= \frac{\omega^2}{8}(1 + \cos(\pi/k)), \\ E_b(t^E_{0,k}) &= \frac{\omega}{2}\cos(\pi/k). \end{aligned} \tag{3.16}$$

The values of $E_{b,\max}$ and $\Sigma^2_{b,\max}$ are plotted in the figure below.

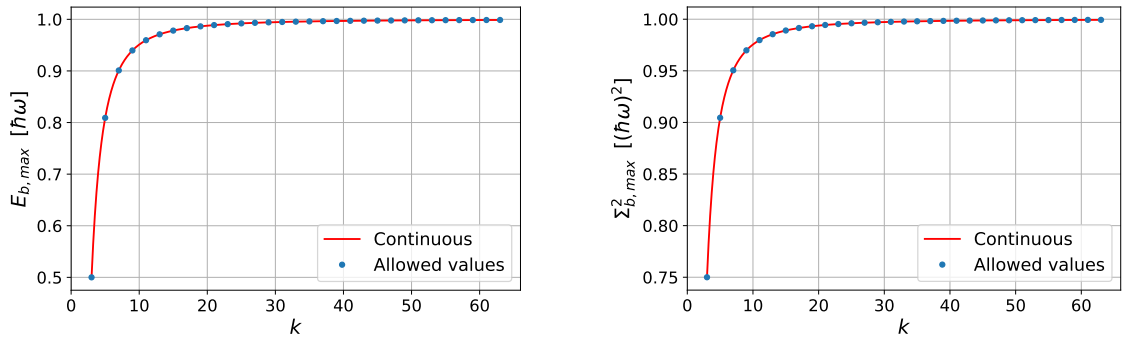

(a) Global maximum of $E_b(t)$.

(b) Global maximum of $\Sigma_b^2(t)$.

Figure 3.1: The global maximum of both the energy (a) and the fluctuations (b) as function of k. In the plots, the maximum values are plotted for both the allowed values (as given in Eq. (3.13)) and continuous values of k. Observe that both plots approach the value 1, which can be justified by taking the limit of $k \to \infty$ for the expressions given in Eq. (3.16). Furthermore, in this plot $\omega = 2$ and $N_b = 2$.

Keep in mind that, as the maxima of both quantities are plotted against k, they are a function of N_c and m as well.
When taking the limit $k \to \infty$ in 3.16 we obtain

$$\lim_{k\to\infty} \Sigma^2(t^{\Sigma}_{0,k}) = \frac{\omega^2}{8}(1+\cos(0)) = \frac{\omega^2}{4},$$
$$\lim_{k\to\infty} E_b(t^{E}_{0,k}) = \frac{\omega}{2}\cos(0) = \frac{\omega}{2} = E_b^{\max}.$$

which explains how both graphs in Fig. (3.1) approach the value 1, as in these graphs ω is set to 2. Note, as indicated in the expression, that the limit value of the energy is its theoretical maximum, given in Eq. (3.2).
For the case $J = 0$, or the case where no nearest-neighbour interactions are present, we find for the same values of n

$$\begin{cases} E_b(t) = -\frac{\omega}{2}\cos(\sqrt{2M}gt) \\ \Sigma^2(t) = \frac{\omega^2}{8}\sin^2(\sqrt{2M}gt) \end{cases} \tag{3.17}$$

where M is the same as defined in Eq. (3.12). M can be written in terms of k as well, which gives $M = (k^2-1)/2$. Notice that in this case, for every allowed value of N_c and m, the battery is always able to be charged to $\omega/2$. As already shown in Eq. (3.16) and Fig. (3.2), this is not the case whenever $J = g = h$. So apparently, the nearest-neighbour interaction together with the fact that $J = g = h$ prevents the battery to be charged to its maximal possible value. What might cause some confusion, is that the energy given in both Eq. (3.16) and (3.17) are cosine functions. However, Eq. (3.16) is the global maximum of the energy as a function of k (and thus of N_c and m), while Eq. (3.17) is the energy as function of time. They cannot be compared and have a different physical interpretation. However, what we can say about these expressions is that for $J = 0$ the maximum value $\omega/2$ can always be reached, as long as we take allowed values of N_c and m according to Eq. (3.13), but this is not the case whenever $J = g = h$ as we can see in Eq. (3.16) and Fig. (3.1). One minor observation that can be made too is that the fluctuations for $J = g = h$ differ by a factor $(\omega^2/4)/(\omega^2/8) = 2$ for $m, N_c \to \infty$ compared

to $J = 0$.
We are also interested in the behaviour of the fluctuations. As mentioned in the introduction, fluctuations are undesired in a quantum battery and thus it is best to have them minimized whenever the battery part is fully charged. In other words, it would be beneficial if the fluctuations have a (local) minimum at the same moment the stored energy has a global maximum. For this we need to check whether, or for what values of k, $\frac{d\Sigma^2}{dt}(t^E_{j,k}) = 0$ and $\frac{d^2\Sigma^2}{dt^2}(t^E_{j,k}) > 0$.
Computing this we find

$$\begin{aligned}\frac{d(\Sigma^2)}{dt}(t^E_{j,k}) &= \frac{h\omega^2(k^2-1)}{16k^2}\left(2\sin(\pm 2\pi/k) + (k+1)\sin(\mp 2\pi/k) + (k-1)\sin(\pm 2\pi/k)\right) \\ &= \frac{h\omega^2(k^2-1)}{16k^2}\left(2\sin(\pm 2\pi/k) - 2\sin(\pm 2\pi/k)\right) = 0\end{aligned}$$

and

$$\begin{aligned}\frac{d^2(\Sigma^2)}{dt^2}(t^E_{j,k}) &= \frac{h^2\omega^2(k^2-1)}{8k^2}\left(2\cos(2\pi/k) + (k^2-1)\cos(2\pi/k) + (k^2-1)\cos(2\pi/k)\right) \\ &= \frac{h^2\omega^2(k^2-1)}{4}\cos(2\pi/k).\end{aligned}$$

Of all the allowed values for k (see 3.13), the last expression is positive for $k \geq 5$, and thus $N_c \geq 4$. Only for $k = 3$ ($N_c = 2$) we have that $\partial^2\Sigma^2/\partial t^2$ is negative. We can conclude that the fluctuations have a (local) maximum for $k = 3$ (or $N_c = 2$) and a (local) minimum for $k \geq 5$ (or $N_c \geq 4$) at $t^E_{i,k}$.
To give an intuition how the energy and its fluctuations evolve over time, for three cases of n the energy and fluctuations are plotted in figure 3.2 below. In the plots, the values of t for which $E_b(t)$ and $\Sigma^2(t)$ have global maxima are marked as well. The three chosen cases are $n = 1$, $n = 2$ and $n = 5$. See the tables A.1 and A.2 in the Appendix for more information on the chosen cases.

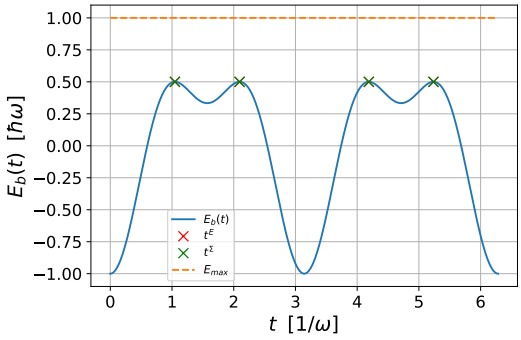

(a) $E_b(t)$ for $n = 1$.

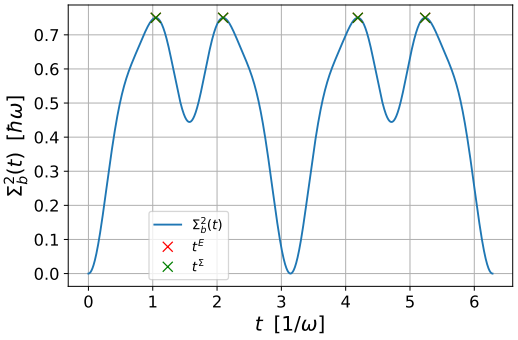

(b) $\Sigma_b^2(t)$ for $n = 1$.

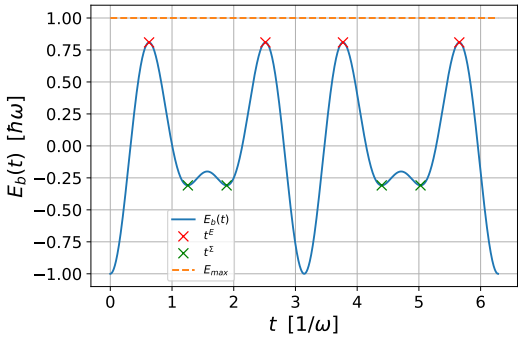

(c) $E_b(t)$ for $n = 2$.

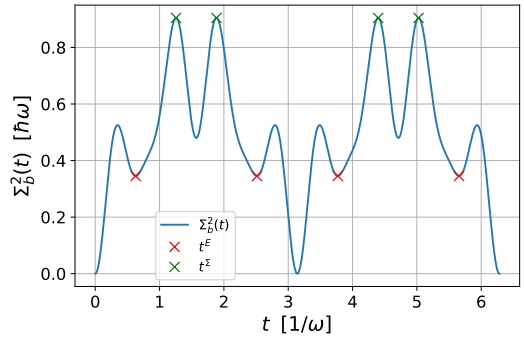

(d) $\Sigma_b^2(t)$ for $n = 2$.

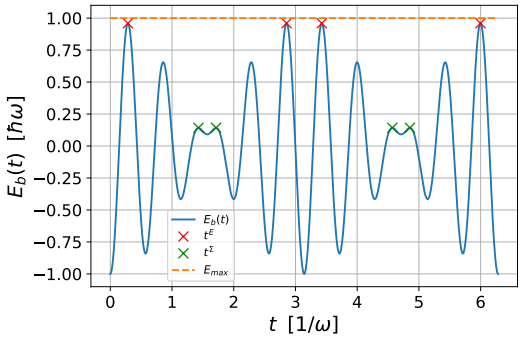

(e) $E_b(t)$ for $n = 5$.

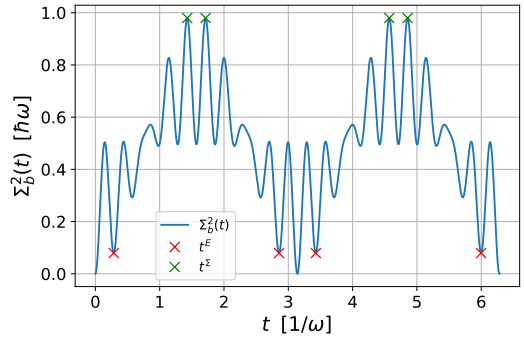

(f) $\Sigma_b^2(t)$ for $n = 5$.

Figure 3.2: The energy and its fluctuations of a central spin battery with 2 battery spins as functions of time. The graph also shows at which values of t both the energy and fluctuations have a global maximum, respectively marked by a red and green $\times$. (a) and (b) shows the energy and fluctuations for $n = 1$, (c) and (d) for $n = 2$ and (e) and (f) for $n = 5$. For more information, see the tables A.1 and A.2 in the Appendix. As already proven, one can see that for the case $n = 1$, $E_b(t)$ and $\Sigma_b^2(t)$ have global maxima for the same values of t, but that the fluctuations have a minimum whenever the energy has a global maximum for $n \geq 2$. Also note that the energy can both have a maximum or a minimum whenever the fluctuations have a global maximum. Furthermore, in this figure $\omega = 2$ and $h = 1$.

As mentioned before, one can see that the period of both functions is not affected by an increase of the size of the system, or by an increase of n or k. However, it is clear that when n is increased, more extrema appear and the global maxima get closer to a fixed point in the period. For the fluctuations, this point is at $\pi/h(j + 1/2)$, and for the energy this point is $\pi j/h$, meaning that the charge time gets smaller when increasing the system size. This last point is true, purely because one of the fixed points of the energy is at $t = 0$, hence the charging time decreases when increasing n.

Also observe that when n is increased, the value of $\Sigma_b^2(t_{j,k}^E)$ decreases. This can be interpreted as whenever the energy gets closer to its theoretical maximum (see 3.2), the fluctuations approaches 0. This happens in two ways: if the energy gets closer to its theoretical maximum in time, but also if it gets closer by increasing n (or k). We can prove this last statement by computing $\Sigma_b^2(t_{i,j}^E)$, which gives

$$\Sigma_b^2(t_{i,j}^E) = \frac{\omega^2}{8}\left(1 - \cos\left(\frac{2\pi}{k}\right)\right). \tag{3.18}$$

and taking the limit $k \to \infty$ (so $N_c, m \to \infty$), to obtain

$$\lim_{k\to\infty} \Sigma_b^2(t_{i,j}^E) = \frac{\omega^2}{8}\left(1 - \cos(0)\right) = 0.$$

This behaviour can also be explained by using the fact that the theoretical maximum is attained whenever $\rho_b(t) = \rho_b^{\max}$. In that case, as already showed, the fluctuations are equal to 0.
Finally, when increasing n, envelopes within the graph of E_b and Σ_b^2 will be more visualised. In figure A.1, the energy and fluctuations for high values of n are plotted. The first thing that can be noticed is that, as already proven, if the envelope of the energy has a maximum, which is automatically its global maximum, the fluctuations has a minimum. As the global maximum of the energy for high values is close to its theoretical maximum, the fluctuations are close to zero. Furthermore, if the envelope of the fluctuations has a maximum, or the fluctuations have a global maximum, then the envelope of the energy has a zero. To proof that the energy approaches zero at $t_{j,k}^{\Sigma}$ when taking $k \to \infty$, we can compute $E_b(t_{j,k}^{\Sigma})$ and take the appropriate limit, giving

$$\lim_{k\to\infty} E_b(t_{j,k}^{\Sigma}) = \lim_{k\to\infty} \left\{\frac{\omega}{2}(-1)^{\frac{k+1}{2}} \sin\left(\frac{\pi}{2k}\right)\right\} = 0 \tag{3.19}$$

Note that this is only true whenever the envelope of the energy has a maximum. The energy has multiple zeros, but most of them do not coincide with a global maximum of the fluctuations (as seen in the example figures 3.2 and A.1). Only the ones that correspond to the zero of the formed envelopes do. This is an important notion which returns later for $N_b > 2$.

3.1.2 Special Case $J \gg g$

For this trivial case, $E_b(t)$ and $\Sigma_b^2(t)$ can be found easily when taking J large enough with respect to g, such that the limit can be approximated to $1 \gg g/J \approx 0$. Assume that this limit is true whenever $J > 100g$. For this limit, the functions in 3.11 reduce to

$$\begin{aligned} \Sigma_b^2(t) &= 0, \\ E_b(t) &= -\frac{\omega}{2}. \end{aligned} \tag{3.20}$$

This means that if the nearest-neighbour interaction, an interaction that takes place between nearest-neighbour battery spins, is large enough compared to flip-flop interaction, which takes place between the battery and charge spins, then the battery is not able to be charged at all, resulting in no fluctuations in the stored energy as well.

3.1.3 Special Case $g \gg J$

Suppose $u^2 = Mg^2$, where M is defined as in Eq. (3.12). Then for the given limit $A = 2Mg^2 + J^2 \approx 2Mg^2$. This simplifies the energy and fluctuations to

$$\begin{cases} \Sigma^2(t) = \frac{\omega^2}{8} \sin^2(\sqrt{2M}gt) \\ E_b(t) = -\frac{\omega}{2} \cos(\sqrt{2M}gt) \end{cases} \tag{3.21}$$

which is the same expression as for the case $J = 0$ seen in Eq. (3.17). This is as expected, because if the flip-flop interaction is large enough such that the nearest-neighbour interaction can be neglected, the battery will behave as one where no nearest-neighbour interaction is present.

3.1.4 Example where $J \neq g$

In this report, no further calculations of $E_b(t)$ and $\Sigma_b^2(t)$ are done for general g and J. This is because the functions of the two mentioned quantities can differ largely for every case of J, g and n. The extrema of $E_b(t)$ can be calculated easily by hand, but they are not particularly consistent in being a minimum or a maximum. However, to check whether some found results from the previous sections are true for $J \neq g$, we can directly calculate the energy and fluctuations by using a specific of J and g. Suppose we take $J = 1$, $g = 2$, $\omega = 2$ and $n = 1$. This gives $m = 2$, $N_c = 2$ and

$$E_b(t) = -\frac{1}{2\sqrt{33}} \left[\left(\sqrt{33}+1\right) \cos\left(\left(\sqrt{33}-1\right)t\right) + \left(\sqrt{33}-J\right) \cos\left(\left(\sqrt{33}+1\right)t\right) \right] \tag{3.22}$$

One of its extrema is at $t = \frac{4\pi}{\sqrt{33}}$, which gives the values

$$\begin{aligned} E_b(t) &= -\frac{1}{2\sqrt{33}} \left[\left(\sqrt{33}+1\right) \cos\left(\left(\sqrt{33}-1\right)\frac{4\pi}{\sqrt{33}}\right) + \left(\sqrt{33}-1\right) \cos\left(\left(\sqrt{33}+1\right)\frac{4\pi}{\sqrt{33}}\right) \right] \\ &\approx 0.99 \end{aligned}$$

This value is much closer to its theoretical maximum given by Eq. (3.2) when comparing it to the case where $J = g = h$. For the same values of N_c and m, it was equal to $\frac{1}{2}$. This means that for $J = g = h$ some sort of resonance occurs that prevents the battery from charging close to its theoretical maximum. Letting the strength of the flip-flop interaction be greater than the nearest-neighbour interaction results in a maximum close to the theoretical maximum.

3.2 Case $N_b > 2$

For this case, numerical calculations are used to check whether the results found in the previous section also apply for systems with more than 2 battery spins. The calculations in this section follow again, as done in section 3.1, the steps given in section 2.3. This time, however all of the calculations are done numerically using Python. See section A.2 for the code. Before showing the results of this section, it is important to have a warning in advance. Due to not having a closed expression for finding the contributions nJ (as already mentioned in section 2.3) and limited computing power, only for a maximum of 24 battery spins the Hamiltonian could be calculated. See table A.3 in the Appendix for the values of these contributions.

3.2.1 Case $J = g = h$

First of all, an interesting result from subsection 3.1.1 was the envelope behaviour of both the energy and its fluctuations. Whenever the energy had a global maximum, the fluctuations had a minimum. Whenever the fluctuations had a global maximum, the energy's envelope had a minimum. This occurred when taking $J = g = h$. To see whether this behaviour also occurs for $N_b > 2$, for the cases $N_b = 4$ and $N_b = 5$ the energy and fluctuations as function of time are plotted below.

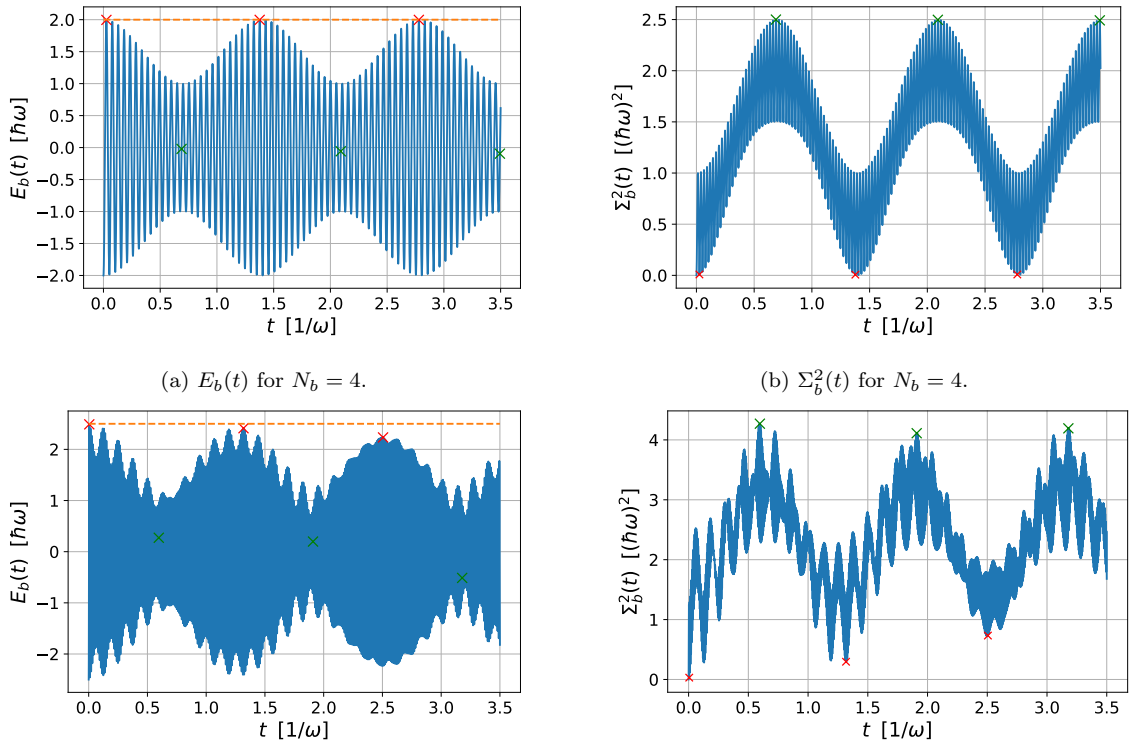

(a) $E_b(t)$ for $N_b = 4$.

(b) $\Sigma_b^2(t)$ for $N_b = 4$.

(c) $E_b(t)$ for $N_b = 5$.

(d) $\Sigma_b^2(t)$ for $N_b = 5$.

Figure 3.3: For two cases the energy and its fluctuations plotted as function of time. The chosen cases are for (a) and (b): $N_b = 4$ and $h = 1$. For (c) and (d) we have $N_b = 5$ and $h = 5$. In both plots $N_c = 120$, $m = 60$ and $\omega = 2$. As for the plots before, the maxima of both the energy and fluctuations are marked with respectively a red and green $\times$. For both cases, envelope behaviour can be seen once more.

In this figure we can again see the envelope behaviour of both the energy and fluctuations. It also can be seen that whenever the envelope of the energy has a maximum (marked with a red $\times$), the envelope of the fluctuations has a minimum. This is precisely in line with the results found for $N_b = 2$. Similar results can be seen the other way around: whenever the envelope of the fluctuations has a maximum, the envelope of the energy has a value close to zero. However, unlike for the case $N_b = 2$, the energy does not have a precise zero. This can be interpreted as follows: whenever the formed envelope of the energy is closest to zero, then the envelope of the fluctuations has a maximum.
From section 3.1.1 we also concluded that if the maximum of the energy's envelope gets closer to its theoretical maximum given by 3.2, the minimum of the fluctuations' envelope gets closer to 0. This can also be seen in Fig. (3.3). Looking carefully, for $N_b = 5$, one can see that the marked maxima of the energy get slightly lower over time in Fig. (3.3c).

This results in an increase of the minimum of the fluctuations' envelope as can be seen in Fig. (3.3d). This can be interpreted that also for $N_b > 2$, the minimum of the envelope of the fluctuations get closer to 0 whenever the maximum of the envelope of the energy get closer to its theoretical maximum. This last mentioned observation will be investigated more clearly momentarily.
Eq. (3.15) showed that the charging time is inversely proportional with h. To check whether this is true for the cases given above, the charging time as function of h is plotted in the figure below. Both cases are plotted in the same figure as their function is almost identical.

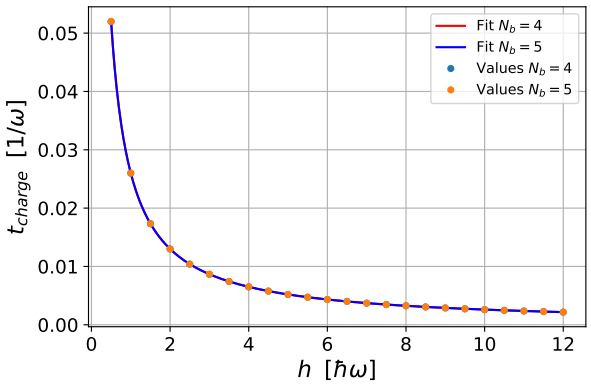

Figure 3.4: Charging time plotted against h. The two chosen cases where $N_b = 4$ and $N_b = 5$. The fitted function used for these plots is $f(x) = a/x$. For both cases, the estimated value of a was approximately 0.0260. Also for both graphs, $N_c = 120$ and $m = 60$.

The charging time for both cases of N_b follow the same graph. This might be due to the small difference in N_b compared to the number of charge spins and spin-ups. What is apparent is how well the graphs lay on the fitted graphs. It shows that for higher values of N_b, the charging time has a inversely proportional relationship with h.
As already mentioned in the analysis of Fig. (3.3), the fact that the minimum of the envelope of the fluctuations gets closer to 0 whenever the maximum of the energy gets closer to its theoretical maximum will be shown more clearly. This will be done by plotting the global maximum of the energy as a function of N_c and m with constant N_b. The following figure consists of such a plot for $N_b = 5$.

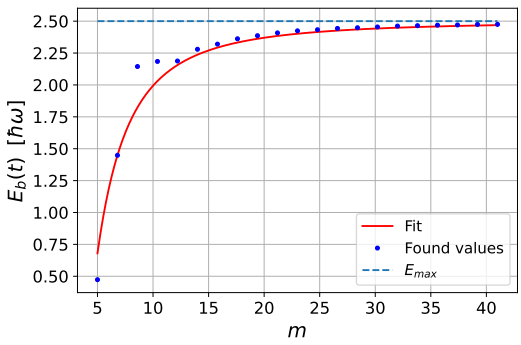

(a) Global maximum of $E_b(t)$ as a function of m.

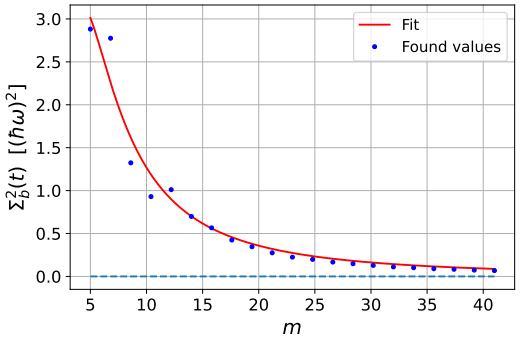

(b) The fluctuations at the same moment in time the energy has a global maximum, as a function of m.

Figure 3.5: This figure shows the maximum energy (a) and the fluctuations at the same moment in time the energy has a maximum, as a function of the number of spin-ups m. In this plot $N_b = 5$, m is ranged from 5 to 41 with steps of 2, $N_c = 2m$, $\omega = 2$ and $h = 1$. The plot also contains a curve-fit, for which similar functions are used as the functions found for the case $N_b = 2$ (second expression in 3.16 and 3.18). The fitted function for the energy is $f(x) = 2.5\cos(b/x)$, with $b \approx 6.48$. The fitted function for the fluctuations is $g(x) = a(1 - \cos(x/b))$, with $a \approx 1.56$ and $b \approx 13.82$. Finally, the figures also shows the predicted limit values. For the energy, this is the theoretical maximum given by 3.2, which in this case is $\frac{5}{2}$. For the fluctuations this is 0.

A similar analysis has been done for a quantum battery consisting of 10 battery spins. The problem with a higher number of battery spins is that the number of charge spins and spin-ups has to be made much higher for the energy to even get over half of its theoretical maximum, when comparing it to cases where N_b is smaller. This can be explained by the fact that for higher numbers of N_b the nearest-neighbour interaction becomes more dominant as the contributions nJ get much higher (as can be seen in table (A.3)). That is why in the following graph the range of m is shifted to much higher values when comparing it to the range in Fig. (3.5).

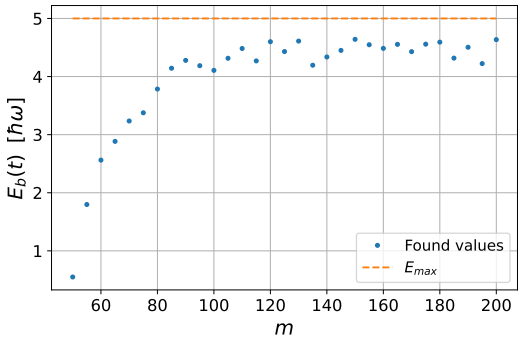

(a) Global maximum of $E_b(t)$ as a function of m.

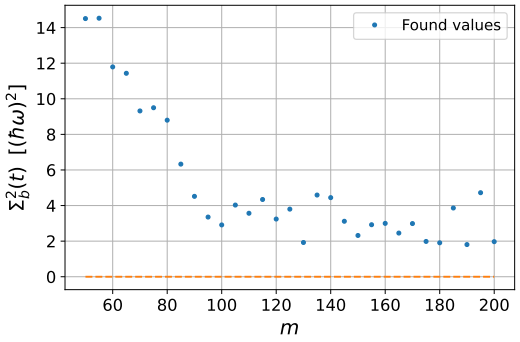

(b) The fluctuations at the same moment in time the energy has a global maximum, as a function of m.

Figure 3.6: This figure shows the maximum energy and the value of the fluctuations at the same moment in time the energy attains its maximum as a function of m. In this figure, $N_b = 10$, m is ranged from 50 to 200 with steps of 5, $N_c = 2m$, $\omega = 2$ and $h = 2$. The plot of the energy also contains the theoretical maximum given by Eq. (3.2), which in this case is equal to 5. The horizontal line in the plot of the fluctuations is the line $\Sigma_b^2 = 0$. Unlike the plots in Fig. (3.5), these plots contain no fitted functions. This is because python was not able to find corresponding parameters for the predicted functions as given in figure 3.5.

We again see the predicted behaviour; the energy increases with the size of the system

(with the increase of m and N_c) and approaches its theoretical maximum $E_b^{\max} = 5$. Simultaneously, the fluctuations drop closer to 0. However, in contrast to Eq. (3.18) and Fig. (3.5), for the case where $N_b = 10$, $E(t)$ is not quite able to reach its theoretical maximum $E_b^{\max} = 5$ and the fluctuations does not completely drop to 0. It also shows much more fluctuations in the values of the plot compared to the case where $N_b = 5$. Important to note is that for this case, no clear envelopes are formed as seen in Fig. (3.3). See Fig. (A.2) for a plot of both the energy and fluctuations for $N_b = 10$.

3.2.2 Varying J

The question arising for the coming two sections is how slight differences in strength of the nearest-neighbour interaction and the flip-flop interaction affect the behaviour of the stored energy and its fluctuations. From section 3.1.2, we can already predict that when taking J/g large enough, the battery is not able to be charged even close to the theoretical maximum of the energy. Especially for systems with a large number of battery spins, the nearest-neighbour interaction can quickly dominate the flip-flop interaction, in the sense that the battery cannot be charged anymore due to the large difference in strength between these two interactions. To demonstrate this, for the case $N_b = 5$ the global maximum of the energy has been plotted as function of J with constant g. See figure 3.7. It also contains a plot of the fluctuations at the moment in time the energy has its global maximum, as a function of J.

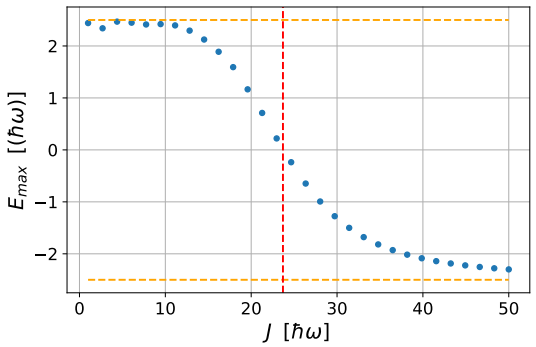

(a) Global maximum of $E_b(t)$ as a function of J.

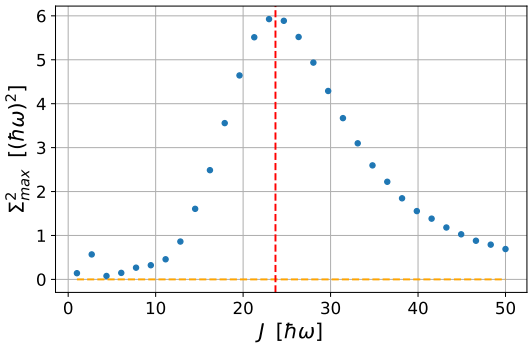

(b) The fluctuations at the same moment in time the energy has a global maximum, as a function of J.

Figure 3.7: This global maximum of the energy (a) and the value of the fluctuations at the same moment in time when the energy has its maximum (b), as function of J and constant g. For this case, $N_b = 5$, $m = 30$, $N_c = 60$, $\omega = 2$, $g = 1$ and J is ranged from 1 to 50. The plot of the energy also contains the lines $E = \pm\frac{5}{2}$ which are respectively its theoretical maximum and minimum, given by Eq. (3.2) and Eq. (3.3). Finally, both figures contain the line $J = 23.7$. This is an estimation for which value of J the graph of the maxima of E_b crosses the J-axis and it shows that it coincides with the peak of the graph of the fluctuations.

In this example, one can see that for the first couple of values of J, the battery is still able to be charged close to its theoretical maximum, which is equal to $\frac{5}{2}$. However, after a certain point somewhere around $J = 12$, the maxima drop and approach the theoretical minimum. Apparent is that the fluctuations has a clear peak. This can be explained by the behaviour of the envelope of the energy whenever the fluctuations has a global maximum, or vice versa. In section 3.1.1, and in particular Fig. (A.1) and Eq. (3.19), we have seen that the envelope of the energy has a zero whenever the envelope

of the fluctuations has a maximum (or whenever the fluctuations has global maximum). This also means that if the energy has a global maximum $E = 0$, and thus the envelope of the energy has a maximum $E = 0$, then the fluctuations reaches its maximum value. This observation can be formulated as follows: the closer the envelope of the energy is to zero, the higher the value of the fluctuations.

3.2.3 Varying g

Previously we saw how the increase of the system for constant N_b affected the maximum achievable value of the energy. This was shown for $N_b = 2$ (Eq. (3.16) and Fig. (3.1a)) and for $N_b > 2$ (Fig. (3.5a) and Fig. (3.6a)). This is not the only method to increase the global maximum of the energy. Another possibility is by increasing g with constant J. The previous section showed that if the nearest-neighbour interaction is strong enough compared to the flip-flop interaction, the battery is not able to be charged much higher than its theoretical minimum. This observation can also be turned around; if we initially have a battery which is not able to be charged due to an improper ratio J/g, we can counter this by increasing g. In this way, the global maximum will increase approaching its theoretical maximum. The following figure shows this behaviour for the case $N_b = 5$. See the caption for more information.

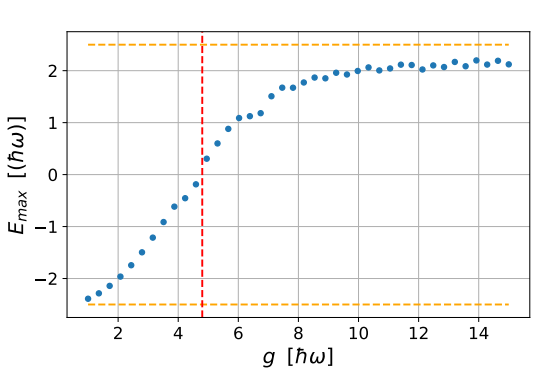

(a) Global maximum of $E_b(t)$ as a function of g.

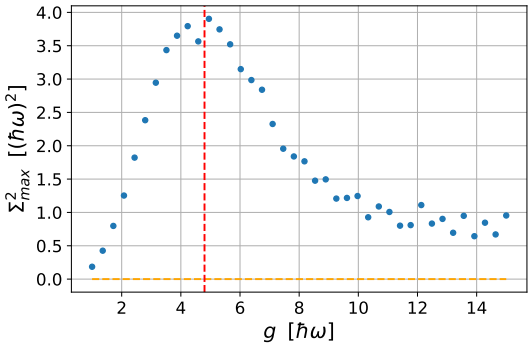

(b) The fluctuations at the same moment in time the energy has a global maximum, as a function of g.

Figure 3.8: This figure shows both the global maximum of the energy (a) and the fluctuations at the same moment in time the energy has a global maximum, as a function of g. For this case, $N_b = 5$, $N_c = m = 8$, $J = 5$, $\omega = 2$ and g is ranged between 1 and 14. (a) also contains the linse $E = \pm\frac{5}{2}$, which are respectively its theoretical maximum and minimum, given by 3.2 and 3.3. (b) contains the line $\Sigma^2 = 0$. Finally, both figures also contain the vertical line $g = 4.8$. This is the estimated value for which the graph of the maximum of E_b crosses the g-axis. It is put in both graphs to demonstrate that the peak of the fluctuations is whenever the maxima of E_b crosses the value $E = 0$.

The figure looks similar to Fig. (3.7), except the plot of the energy 3.8a is mirrored along the g-axis when comparing it to figure 3.7a. This difference in figure is as predicted: at first, we have the ratio $J/g > 1$, which results in the lack of ability of the battery to be charged. In that case, both the energy and fluctuations are close to zero. However, when increasing g, and thus the coupling between the battery- and charge-spins, the global maximum increases. As the global maximum of the energy approaches and surpasses 0, the fluctuations form a peak. This behaviour was already recognised and explained in the previous case, using results from the section where $N_b = 2$. Note however, that the

energy is not quite able to truly reach the theoretical maximum. This can be a result from not having sufficient charge-spins and spin-ups.

Chapter 4

Conclusions and Recommendations

4.1 Conclusions

In this thesis the stored energy and its fluctuations of a central spin battery with nearest-neighbour interaction between the battery spin is calculated and analysed. For a system with 2 battery spins, these calculations are done analytically. For $N_b > 2$, these calculations were done numerically using python.

For $N_b = 2$, the simplification was used that $\omega_b = \omega_c \equiv \omega$ and $u_1 = u_2 \equiv u$. The former assumption meant that the energy splitting for both the battery and charge spins were equal. The latter one does not necessarily have a unambiguous physical meaning, but it adds a constraint to the number of spin-ups m and charge spins N_c, given by $N_c = 2(m-1)$. Using these simplifications and defining $J = g \equiv h$, meaning that the strength of the nearest-neighbour and flip-flop interaction were equal, we could show that the global maximum of both the energy and fluctuations was dependent on the number of charge spins and spin-ups. This stood in contrast to the case where no nearest-neighbour interactions were present (or where $J = 0$), in which case the maximum was always equal to the theoretical maximum. However, the limit $N_c, m \to \infty$ of the energy for $J = g = h$ gave the expected theoretical maximum.
Using the values of t for which the energy had a global maximum, it could be seen that the charge time of the battery is inversely proportional to both h and k, where $k = N_c + 1 = 2m - 1$.
What was shown too, is that for $N_c \geq 4$ the fluctuations had a minimum whenever the function of the energy had a global maximum, taking only the allowed values for m and N_c according to the constraint following from the simplification.
Taking higher values of N_c and m, envelopes were formed for both the energy and fluctuation as function of t. Observing these formed envelopes, it was clear that the fluctuations had a global maximum whenever the envelope of the energy had a zero.
The limit $J \gg g$ resulted in a battery that could not be charged at all, and which fluctuations remained 0 for all t. This could be explained by the fact that whenever $J \gg g$, the nearest-neighbour interaction dominated the flip-flop interaction resulting in no possibility for the battery to be charged. Taking the limit $g \gg J$, the battery could be approached as one where no nearest-neighbour interaction is present, giving the same results as when $J = 0$.
Finally, letting the strength of the flip-flop interaction be twice the strength of the nearest-

neighbour interaction resulted in a maximum much closer to the theoretical maximum compared to the case where $J = g = h$, for the same number of spin-ups and charge spins. No direct explanation was found for why the battery is not able to be charged close to its theoretical maximum when taking $J = g = h$, when comparing it to taking $g = 2J$ with the same number of charge spins and spin-ups. A reason could be that the system is arranged in such a way, that a certain resonance occurs which prevents the battery to be charged closer to its theoretical maximum.
For $N_b > 2$, similar results were found. For $J = g = h$ and the chosen cases of N_b, envelopes formed that showed similar behaviour as for the case $N_b = 2$; the envelope of the energy had maxima whenever the envelope of the fluctuations had minima, and the fluctuations had global maxima whenever the envelope of the energy was closest to 0.
Again, for the chosen cases, the charging time was inversely proportional to h.
Plotting the global maximum of the energy as a function of m and N_c, it was shown that for $N_b > 2$ the global maximum was dependent on the size of the system (with constant N_b), which graph looked similar to the one of the case $N_b = 2$. A plot of the fluctuations at the same moment in time the energy had a global maximum showed that whenever the energy was closer to its theoretical maximum, the fluctuations was closer to 0.
Furthermore, in this section, it was also investigated when J and g differed from each other without directly falling into the limiting cases (as those given in the section in which $N_b = 2$). When varying J, it could be seen that increasing J did not have any effect on the global maximum of the energy until a certain turning point, which made the global maximum drop from its theoretical maximum to its theoretical minimum. The fluctuations at the same moment in time the energy had its global maximum showed that a peak formed when the global maximum of the energy crossed the line $E = 0$. This could be explained by the behaviour we saw previously: the fluctuations have a maximum whenever the envelope of the energy has a zero. So if the energy has a global maximum $E_{\max} = 0$, then the envelope of the energy has a zero (as its global maximum is a zero), resulting in the fluctuations to have a maximum.
Varying g gave similar results as the previous observation. Starting with a situation where a battery could not be charged much more than its theoretical minimum due to an improper ratio $J/g > 1$, the global maximum could be increased to its theoretical maximum by increasing g. Again, the global maximum of the energy crossed the line $E = 0$, which resulted in a peak for the fluctuations. This could be explained by the same reason as given by the previous observation.

4.2 Recommendations

For further research, multiple paths can be taken. First, the origin of the lower global maximum for $J = g = h$, compared to the case where $J = 0$ could be investigated. For this, the analytical expressions in 3.11 could be used and letting $g = (1 + \epsilon)J$, with some number $\epsilon > 0$. Using the limit $\epsilon \to 0$, the behaviour of the energy and fluctuations could be analysed from which a conclusion might be taken why this behaviour occurs. Furthermore, a reason for the maximum of the fluctuations whenever the envelope of the energy has a zero may be found by studying the relationship between the fluctuations and the occupation given by the reduced density matrix.
To extend the research, one could investigate the influence of decoherence on the system. This can be done by introducing the Lindblad operator in the master equation [2].

Bibliography

[1] Christian Arenz, Giulia Gualdi, and Daniel Burgarth. Control of open quantum systems: case study of the central spin model. *New Journal of Physics*, 16(6): 065023, June 2014. ISSN 1367-2630. doi: 10.1088/1367-2630/16/6/065023. URL http://dx.doi.org/10.1088/1367-2630/16/6/065023.

[2] Mohammad B. Arjmandi, Hamidreza Mohammadi, and Alan C. Santos. Enhancing self-discharging process with disordered quantum batteries. *Physical Review E*, 105 (5), May 2022. ISSN 2470-0053. doi: 10.1103/physreve.105.054115. URL http://dx.doi.org/10.1103/PhysRevE.105.054115.

[3] A Crescente, M Carrega, M Sassetti, and D Ferraro. Charging and energy fluctuations of a driven quantum battery. *New Journal of Physics*, 22(6):063057, Jun 2020. doi: 10.1088/1367-2630/ab91fc.

[4] Fu-Quan Dou and Fang-Mei Yang. Superconducting transmon qubit-resonator quantum battery. *Phys. Rev. A (Coll. Park.)*, 107(2), February 2023.

[5] David J Griffiths and Darrell F Schroeter. *Introduction to Quantum Mechanics*. Cambridge University Press, Cambridge, England, 3 edition, August 2018.

[6] David Jen. What quantum batteries have in store, Jun 2022. URL https://semiengineering.com/what-quantum-batteries-have-in-store/.

[7] Ryan Larose. Quantum states and partial trace, 2018. URL https://www.ryanlarose.com/uploads/1/1/5/8/115879647/quic06-states-trace.pdf.

[8] Jia-Xuan Liu, Hai-Long Shi, Yun-Hao Shi, Xiao-Hui Wang, and Wen-Li Yang. Entanglement and work extraction in the central-spin quantum battery. *Physical Review B*, 104(24), December 2021. ISSN 2469-9969. doi: 10.1103/physrevb.104.245418. URL http://dx.doi.org/10.1103/PhysRevB.104.245418.

[9] James Millen and André Xuereb. Perspective on quantum thermodynamics. *New Journal of Physics*, 18(1):011002, jan 2016. doi: 10.1088/1367-2630/18/1/011002. URL https://dx.doi.org/10.1088/1367-2630/18/1/011002.

[10] John Schliemann, Alexander Khaetskii, and Daniel Loss. Electron spin dynamics in quantum dots and related nanostructures due to hyperfine interaction with nuclei. *Journal of Physics: Condensed Matter*, 15(50):R1809–R1833, December 2003. ISSN 1361-648X. doi: 10.1088/0953-8984/15/50/r01. URL http://dx.doi.org/10.1088/0953-8984/15/50/R01.

[11] Wang Yao, Ren-Bao Liu, and L. J. Sham. Theory of electron spin decoherence by interacting nuclear spins in a quantum dot. *Physical Review B*, 74(19), November 2006. ISSN 1550-235X. doi: 10.1103/physrevb.74.195301. URL http://dx.doi.org/10.1103/PhysRevB.74.195301.

[12] Fang Zhao, Fu-Quan Dou, and Qing Zhao. Quantum battery of interacting spins with environmental noise. *Physical Review A*, 103(3), March 2021. ISSN 2469-9934. doi: 10.1103/physreva.103.033715. URL http://dx.doi.org/10.1103/PhysRevA.103.033715.

Appendix A

Appendix

A.1 Additional Graphs and Tables

(n, m, N_c, k)	$E_b(t) =$	$t_{\max}=$	$E_{b,\max} =$
$(1, 2, 2, 3)$	$-\frac{\omega}{6}(2\cos(2ht) + \cos(4ht))$	$\frac{\pi}{h}\left(j \pm \frac{1}{3}\right)$	$\omega/4$
$(2, 3, 4, 5)$	$-\frac{\omega}{10}(3\cos(4ht) + 2\cos(6ht))$	$\frac{\pi}{h}\left(j \pm \frac{1}{5}\right)$	$\frac{\omega}{8}(1+\sqrt{5})$
$(5, 6, 10, 11)$	$-\frac{\omega}{22}(6\cos(10ht) + 5\cos(12ht))$	$\frac{\pi}{h}\left(j \pm \frac{1}{11}\right)$	$\approx 0.480\omega$

Table A.1: Information about E_b for the three cases plotted in figure 3.2 in section 3.1.1. For each case, the table contains the values of $n,\ m,\ N_c$, and k, the function $E_b(t)$, the values of t for which it contains a global maximum, and it contains its function value at the global maximum. For all three cases, $J = g = h$ and $N_b = 2$.

(n, m, N_c, k)	$\Sigma_b^2(t) =$	$t_{\max} =$	$\Sigma_{b,\max}^2 =$
$(1, 2, 2, 3)$	$\frac{\omega^2}{72}(9 - 4\cos(2ht) - 4\cos(4ht) - \cos(8ht))$	$\frac{\pi}{h}\left(j + \frac{1}{2}(1 \pm \frac{1}{3})\right)$	$3\omega^2/16$
$(2, 3, 4, 5)$	$\frac{\omega^2}{200}(25 - 12\cos(2ht) - 9\cos(8ht) - 4\cos(12ht))$	$\frac{\pi}{h}\left(j + \frac{1}{2}(1 \pm \frac{1}{5})\right)$	$\frac{\omega^2}{32}(5+\sqrt{5})$
$(5, 6, 10, 11)$	$\frac{\omega^2}{968}(121 - 60\cos(2ht) - 36\cos(20ht) - 25\cos(24ht))$	$\frac{\pi}{h}\left(j + \frac{1}{2}(1 \pm \frac{1}{11})\right)$	$\approx 0.245\omega^2$

Table A.2: Information about Σ_b^2 for the three cases plotted in figure 3.2 in section 3.1.1. For each case, the table contains the values of $n,\ m,\ N_c$, and k, the function $\Sigma_b^2(t)$, the values of t for which it contains a global maximum, and it contains its function value at the global maximum. For all three cases, $J = g = h$ and $N_b = 2$.

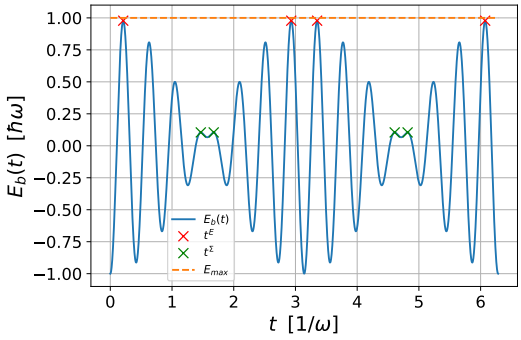

(a) $E_b(t)$ for $n = 7$.

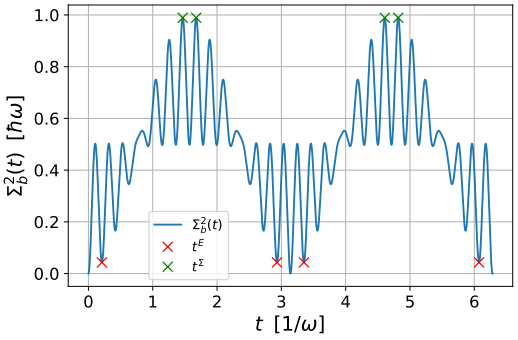

(b) $\Sigma_b^2(t)$ for $n = 7$.

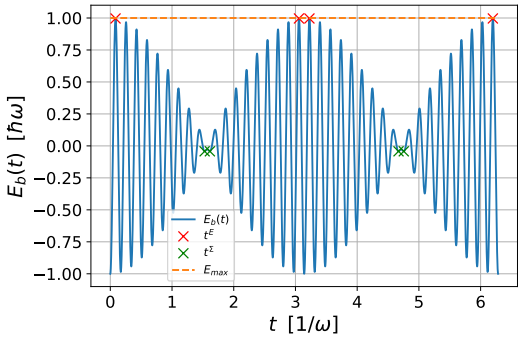

(c) $E_b(t)$ for $n = 18$.

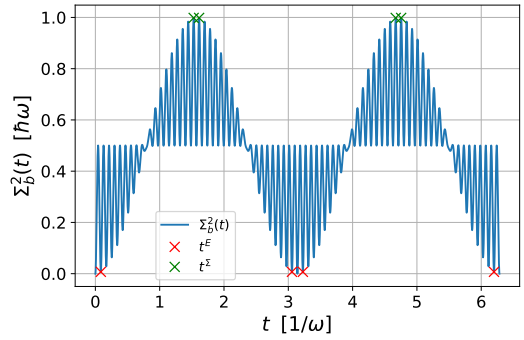

(d) $\Sigma_b^2(t)$ for $n = 18$.

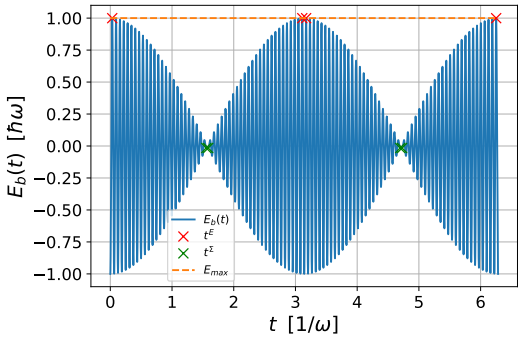

(e) $E_b(t)$ for $n = 50$.

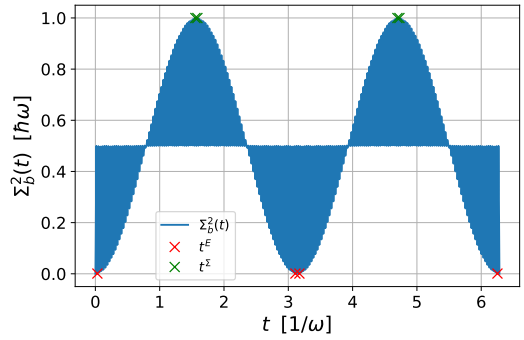

(f) $\Sigma_b^2(t)$ for $n = 50$.

Figure A.1: The energy and its fluctuations as functions of time for $N_b = 2$. The graph also shows at which values of t both the energy and fluctuations has a global maximum, respectively marked by a red and green $\times$. (a) and (b) shows the energy and fluctuations for $n = 7$ ($m = 8$, $N_c = 14$), (c) and (d) for $n = 18$ ($m = 19$, $N_c = 36$) and (e) and (f) for $n = 50$ ($m = 51$, $N_c = 10$). The plots of the energy also shows the theoretical maximum as given in Eq. (3.2). The higher n gets, the more clear one can see the formation of envelopes. Furthermore, in this figure $\omega = 2$ and $h = 1$.

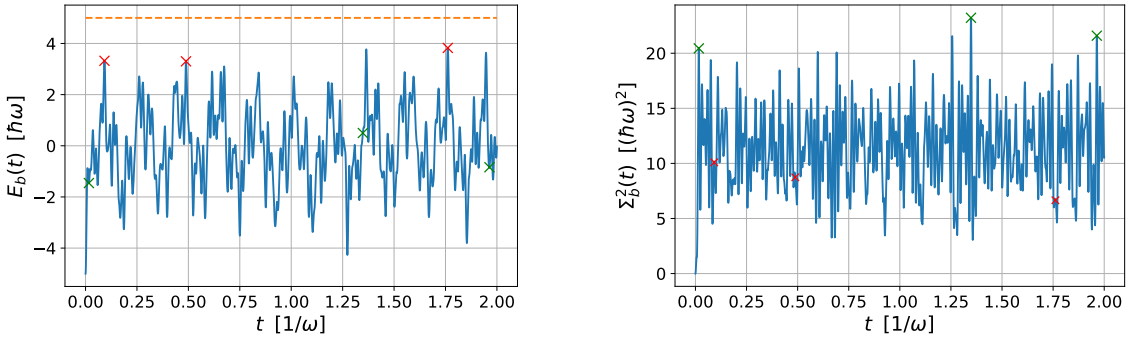

(a) $E_b(t)$. (b) $\Sigma_b^2(t)$.

Figure A.2: The energy and its fluctuations as functions of time. The graph also shows at which values of t both the energy and fluctuations have a global maximum, respectively marked by a red and green $\times$. In this case, $N_b = 10$, $m = 100$ and $N_c = 200$. Furthermore, in this figure $\omega = 2$ and $J = g = h = 1$. The graph shows that for higher values of N_b no clear envelopes are formed anymore.

N	$m=1$	$m=2$	$m=3$	$m=4$	$m=5$	$m=6$	$m=7$	$m=8$	$m=9$	$m=10$	$m=11$	$m=12$
2	2											
3	4											
4	6	12										
5	8	24										
6	10	40	60									
7	12	60	120									
8	14	84	210	280								
9	16	112	336	560								
10	18	144	504	1008	1260							
11	20	180	720	1680	2520							
12	22	220	990	2640	4620	5544						
13	24	264	1320	3960	7920	11088						
14	26	312	1716	5720	12870	20592	24024					
15	28	364	2184	8008	20020	36036	48048					
16	30	420	2730	10920	30030	60060	90090	102960				
17	32	480	3360	14560	43680	96096	160160	205920				
18	34	544	4080	19040	61880	148512	272272	388960	437580			
19	36	612	4896	24480	85680	222768	445536	700128	875160			
20	38	684	5814	31008	116280	325584	705432	1209312	1662804	1847560		
21	40	760	6840	38760	155040	465120	1085280	2015520	3023280	3695120		
22	42	840	7980	47880	203490	651168	1627920	3255840	5290740	7054320	7759752	
23	44	924	9240	58520	263340	895356	2387616	5116320	8953560	12932920	15519504	
24	46	1012	10626	70840	336490	1211364	3432198	7845024	14709420	22881320	29745716	32449872

Table A.3: This table contains all values of the contributions n_j, necessary for the Hamiltonian in matrix form (2.18). All values are calculated using a python program. The table works as follows: the rows indicate what size of the system you are working in and the columns indicate the number of spin-ups of the given Dicke state (2.6). E.g., the state $|5\rangle$ for $N = 16$, has a total contribution $n_5 = 30030$. For each system with size N, only half of the values n_j are given. This is because the number of contributions is symmetric. Suppose we have an even number N spins of which m are spin-up. Then $N - m$ spins are spin-down. This gives the same number of contributions n_m as if we turned the situation around: so $N - m$ spin-ups and m spin down. This is because both situations produce the same permutations of states, except all spins are opposite oriented. This does not affect the total number of reversals, as it only matters if two nearest-neighbour spins are opposite oriented. A similar analysis can be done for an odd number of spins.

A.2 Code

This section only contains the main code used for this thesis. All evaluation code e.g. the code used to make the figures, can be found on https://github.com/olivierkokkedee/BEP-quantum-battery. As already mentioned in the README.md file, the code might not contain all code used for the evaluation of the data, as it may already be deleted. It may also contain code that is used nowhere in this thesis.

```
import numpy as np
import matplotlib.pyplot as plt
from itertools import combinations
import pandas as pd
import math
import os
os.chdir('private')
from scipy.optimize import curve_fit

#Defining all parameters
h=1
n=60
Nb=5
Nc=8
m=8
k=2*n+1
J=5
omega_b=2
omega_c=2
g=10
M=2*m*(Nc-m+1)
A=2*M*g**2+J**2

t_end=10
t_steps=5000
t=np.linspace(0,t_end,t_steps+1)
ftsize=16

#%matplotlib inline
#Opening the excel file which contains all contribution values n for certain
    states
df = pd.read_excel('private')
nJ_contribution = df.iloc[:, 1:].to_numpy()

#u_j and b_j, as they are defined in Liu et al.
def u(j, Nb, Nc, m, J, omega_b, omega_c, g):
    return g * np.sqrt(j * (Nb - j + 1) * (Nc - m + j) * (m - j + 1))

def b(j, Nb, Nc, m, J, omega_b, omega_c, g):
    return omega_b / 2 * (j - Nb / 2) + omega_c / 2 * (m - j - Nc / 2)

#creating the array which contains all contributions nJ, so I can add it to
```

```
    the Hamiltonian later
def get_nJ_diagonal(Nb):
    diagonal = np.array([0]) # Start with a single element, 0

    if (Nb - 2) % 2 == 0:
        for i in range(1, int(Nb / 2) + 1):
            diagonal = np.append(diagonal, nJ_contribution[Nb - 2, i - 1])
        diagonal = np.concatenate((diagonal, diagonal[-2::-1]))
    else:
        for i in range(1, int(math.floor(Nb / 2)) + 1):
            diagonal = np.append(diagonal, nJ_contribution[Nb - 2, i - 1])
        diagonal = np.concatenate((diagonal, diagonal[::-1]))

    return diagonal

#the following functions calculate the intermediate steps to calculate the
    energy and fluctuations
def total_hamiltonian(Nb, Nc, m, J, omega_b, omega_c, g):
    nJ_diag=get_nJ_diagonal(Nb)
    u_arr = [u(j + 1, Nb, Nc, m, J, omega_b, omega_c, g) for j in range(Nb)]
    b_arr = [b(j, Nb, Nc, m, J, omega_b, omega_c, g) for j in range(Nb + 1)]
    b_arr=b_arr+nJ_diag*J
    H = np.diag(b_arr) + np.diag(u_arr, k=1) + np.diag(u_arr, k=-1)
    return H

def H_b(Nb,omega_b):
    diagonal=[omega_b/2*(j-Nb/2) for j in range(Nb+1)]
    Hb=np.diag(diagonal)
    return Hb

def state_psi(t, Nb, Nc, m, J, omega_b, omega_c, g):
    H = total_hamiltonian(Nb, Nc, m, J, omega_b, omega_c, g)
    eigenvalues, eigenvectors = np.linalg.eig(H)
    normalized_eigenvectors = np.array([v / np.linalg.norm(v) for v in
        eigenvectors.T]).T
    U = normalized_eigenvectors
    D = np.diag(np.exp(-1j * eigenvalues * t))
    A = np.dot(U, np.dot(D, U.conj().T))

    x = np.zeros((Nb + 1, 1))
    x[0] = 1
    return np.dot(A, x)


def reduced_density(t, Nb, Nc, m, J, omega_b, omega_c, g):
    rho_b=np.zeros((Nb+1,Nb+1))
    psi=state_psi(t, Nb, Nc, m, J, omega_b, omega_c, g)
    for i in range(Nb+1):
        rho_b[i,i]=abs(psi[i,0])**2
    return rho_b
```

```
def E_t(t, Nb, Nc, m, J, omega_b, omega_c, g):
    rho_b=reduced_density(t, Nb, Nc, m, J, omega_b, omega_c, g)
    Hb=H_b(Nb,omega_b)
    return np.dot(Hb,rho_b).trace()

def fluctuations(t, Nb, Nc, m, J, omega_b, omega_c, g):
    Et=E_t(t, Nb, Nc, m, J, omega_b, omega_c, g)
    Hb=H_b(Nb, omega_b)
    rho_b=reduced_density(t, Nb, Nc, m, J, omega_b, omega_c, g)
    Hb_sq=np.dot(Hb,Hb)
    A=np.dot(Hb_sq,rho_b)
    return A.trace()-Et**2
```